Design of Integrated Crystallization Systems

Christianto Wibowo, Wen-Chi Chang, and Ka M. Ng
Dept. of Chemical Engineering, University of Massachusetts, Amherst, MA 01003

A systematic procedure is developed for designing an integrated crystallization system by considering the interaction between crystallization and downstream processing. Potential problems related to unit operations such as filtration, washing, dewatering, recrystallization, and drying are anticipated and resolved by determining an operating policy and configuration for the crystallizer as well as the downstream units. The approach can be applied to both batch and continuous crystallizers. First, the possible impacts of particle-size distribution (PSD) on the downstream processing units are identified. This forms the basis for determining a target PSD in the second step. Third, possible means by which the desired PSD can be achieved are selected. Fourth, the alternatives thus generated are evaluated and compared to identify the best design. Heuristics are provided along the way to guide the decision making. Shortcut equipment models are used to compare the performance of the alternatives. The procedure is illustrated with two industrial examples, including the production of adipic acid.

Introduction

Crystallization finds many applications in the chemical process industries, especially those involving solid products and/or solids processing. Examples include the manufacture of inorganic salts, detergents, fertilizers, insecticides, herbicides, and pharmaceuticals. Much is known about crystallization fundamentals (Bamforth, 1965; Jančić and Grootscholten, 1984; Rousseau, 1987; Randolph and Larson, 1988; Nývlt, 1992; Sohnel and Garside, 1992; Mullin, 1993; Myerson, 1993; Tavare, 1991, 1995). Recently, there also has been a great deal of interest in examining crystallization systems from the perspective of process systems engineering. The aim is to come up with a reliable, optimal process while minimizing development time and effort.

Specifically, procedures for synthesis of crystallization-based separation systems have been formulated (Cisternas and Rudd, 1993; Dye and Ng, 1995a,b; Berry and Ng, 1996, 1997; Berry et al., 1997; Takano et al., 1999; Schroer et al., 2001). Various crystallization techniques, such as extractive crystallization, fractional crystallization, and drowning out crystallization, and different materials ranging from organic, ionic, to chiral compounds, have been considered. Recently, a unified procedure for synthesizing crystallization flow sheets regardless of crystallization technique and material was proposed (Wibowo and Ng, 2000). Given the separation objective and the phase diagram of the system on hand, flow sheet alternatives can be systematically constructed by considering the separation steps in a flow sheet as movements on a phase diagram.

Chang and Ng (1998) extended the synthesis procedure for crystallization systems to include the processing system around a crystallizer. This is important because a crystallizer does not exist in isolation in a chemical plant. Downstream of the crystallizer, filters, dissolvers, washing tanks, recrystallizers, and dryers are used to separate, clean, and dry the product crystals. The procedure guides the user to configure the streams containing reaction solvent, drowning-out solvent, mother liquor, wash liquid, and recrystallization solvent so as to improve process efficiency of such a downstream crystallization system. However, problems related to product quality and operations have not yet been fully considered.

Indeed, despite all the progress, solid–liquid separation downstream of the crystallizer can still be troubled by various operational problems. For example, the crystallizer may produce an excess amount of fine crystals, resulting in low cake permeability and difficult filtration (Jones, 1985). This can lead to an unacceptably long filtration time in a batch process, or the need for an exceedingly large filter area in a continuous process. Another problem is the presence of impurities in the product beyond an acceptable level, such that extensive washing or even a costly recrystallization step is nec-

Correspondence concerning this article should be addressed to K. M. Ng at the Dept. of Chemical Engineering, Hong Kong University of Science and Technology, Clear Water Bay, Hong Kong.

essary. It should be recognized that these problems originate in the crystallizer.

In fact, the crystallizer and the downstream processing systems are highly coupled, particularly through the particle-size distribution (PSD). Rajagopal et al. (1988) identified an optimum dominant crystal size resulting from a trade-off between crystallizer and filter costs. Rossiter and Douglas (1986) showed that the residual moisture content in the centrifuge, and thus the drying cost, is affected by crystal size. Simulation studies using population balance equations demonstrated the importance of recycled seed crystals in an alumina plant (Hill and Ng, 1997). While downstream processing problems can be handled by modifying the filters and dryers, it is far simpler to eliminate the potential problems in the crystallizer. Modifications to an upstream crystallizer, such as operating the crystallizer under different policies (Garside, 1985; Tavare, 1995) or using a different crystallization solvent (Myerson et al., 1986), can lead to a different PSD. For example, Jones et al. (1987) presented experimental data showing that the filterability of potassium sulfate crystals was improved by performing the batch crystallization with a different cooling rate. As pointed out by Bermingham et al. (2000), it is highly desirable to take into account the downstream processing issues such as filterability and washability while designing the crystallizer.

This article presents a systematic design procedure to identify and resolve PSD-related issues in an integrated crystallization system. Potential problems related to downstream units such as filtration, washing, deliquoring, crystal purity, drying, and so on are anticipated and resolved by modifying the operation of the crystallizer, if possible, as well as the downstream units, if necessary. It is applicable for designing a new plant as well as retrofitting an existing one, with batch or continuous crystallizers.

Systematic Procedure for Designing an Integrated Crystallization System

The procedure consists of four steps. First, the possible impacts of PSD on the downstream processing units are identified. Second, analyses are performed to determine the target PSD to avoid or resolve the potential problems. Third, practical ways to resolve the problem are explored. These include modifications of the upstream crystallizer operating policies and of the downstream units. Fourth, the alternatives thus generated are evaluated and compared to identify the best design. Heuristics are provided for each step along with quantitative models to guide the decision making.

The procedure is predicated on the following assumptions. The reaction system, if used before the crystallization step, is assumed to be fixed. Thus, the composition of the feed stream to the crystallizer is known. The product purity and production rate are specified. Experimental data on crystallization kinetics, solubility, and impurity inclusion formation are available.

Step 1: identification of potential problems related to PSD

The generic structure of the processing units downstream of a crystallizer is depicted in Figure 1. The crystals leaving the crystallizer are first separated from the mother liquor.

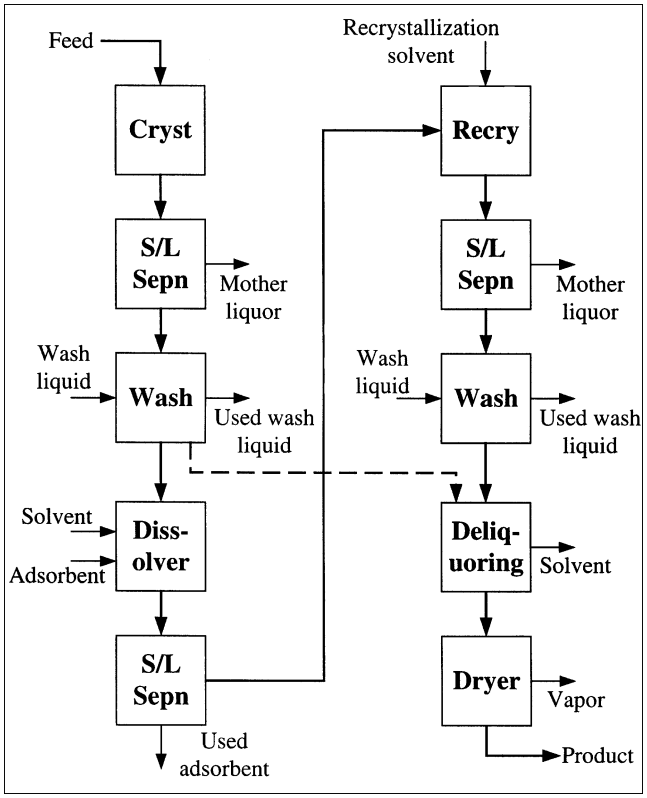

Figure 1. General structure of crystallization downstream processing system.

The crystals are then washed to remove dissolved impurities trapped in the void space. If the crystal size or shape does not meet the product requirements, or if the amount of impurity inclusion is unacceptable, a recrystallization step may be necessary. If this is the case, the crystals are dissolved and an adsorbent is added to the solution to remove impurities. After recrystallization, the resultant crystals are again separated and washed. To remove the trapped liquid in the void space, a deliquoring step is performed before drying. Decisions regarding the units to be used and the destinations of all side streams can be made following the synthesis procedure of Chang and Ng (1998). In some situations, the entire crystallization–washing–deliquoring–drying train can be replaced by a spray dryer. This solid–liquid separation train is typically followed by the bulk-solids processing step, where final product specifications, such as size, shape, and composition, are met (Wibowo and Ng, 1999, 2001).

Table 1 presents some of the potential problems in crystallization downstream units. It emphasizes those in the solid–liquid separation units, but also includes problems related to compaction and pneumatic transport in the bulk solids processing step. Most of the root problems can be traced to an improper PSD for the unit under consideration. The PSD may contain too many fines, too broad, or too narrow, and the average particle size may be too large or too small. Other problem sources unrelated to PSD are also identified in the last column of Table 1, although their treatment is beyond the scope of this study. For example, let us

consider potential filtration problems. An unacceptably long filtration time in a batch filter can be caused by a wide PSD or a small average particle size. The former results in a lower cake porosity that, along with small particles, leads to a low filter cake permeability. Fines can also clog the filter medium, such that the filter-medium resistance increases drastically. However, difficult filtration can also be caused by a highly compressible filter cake, which cannot be rectified by changing the PSD.

Some potential problems may arise because of the operation limitations of a continuous unit. For example, the time available for washing and deliquoring in a rotary drum filter depends on the fraction of the drum surface (f_a) devoted to each function. The available time, t_a, is simply

$$t_a = \frac{2\pi f_a}{\omega}, \tag{1}$$

where ω is the rotational speed of the filter. It is necessary to keep the washing and deliquoring time smaller than the available time to ensure that the operation can be completed.

Another commonly encountered problem is crystal purity. During crystal growth, small pockets of mother liquor are often trapped in the crystal interior, forming inclusions. Since the mother liquor contains the solvent and other solutes as well, inclusions have a significant effect on crystal quality. Once formed, inclusions cannot be removed using washing and deliquoring, and recrystallization is the only way to purify the crystals.

If there is a dissolution step downstream of the crystallizer, the presence of large particles may lead to a long dissolution time (Hill and Ng, 1997). If the crystals are to be sent to a compactor for size enlargement, a narrow PSD is undesirable, because the resulting agglomerate may not have sufficient strength (Pietsch, 1991). If pneumatic conveyors are used for transportation of the dry crystals, a wide PSD can lead to undesired demixing or classification. Also, fines may stick to the walls and end up clogging the pneumatic line. In fact, deposition is also a potential problem in many other units, such as mixers, screens, and crushers (Wibowo and Ng, 2001). Regardless of size, solid particles attach to the walls more easily in the presence of moisture. Therefore, the hygro-

Table 1. Potential PSD-Related Problems in Crystallization Downstream Processing

Potential Problems	Possible PSD-Related Sources: Too Much Fines	PSD Too Wide	PSD Too Narrow	Average Size Too Small	Average Size Too Large	Other Possible Sources
Filtration						
Batch filtration is too long, or required continuous filter area is too large		√		√		The cake is highly compressible.
Filter system, including the filter medium, is easily clogged	√					—
Washing						
Solvent requirement is too high, leading to expensive recovery cost		√		√		The impurity adsorbs strongly on the crystals.
Required washing time is too long, or larger than what is available in a continuous filter		√		√		The cake is highly compressible
Recrystallization						
Impurity inclusion level is too high, such that recrystallization is necessary					√	Crystal growth rate is too fast.
Deliquoring						
Deliquoring time to achieve a specified saturation level is too long, or larger than what is available in a continuous filter		√		√		The cake is highly compressible.
Residual liquid content of the cake is too high	√		√			—
Drying						
Required drying time is too long and energy consumption is too high		√		√		—
Too much dust in the drying system	√					—
Dissolution						
Dissolution time is too long		√			√	—
Compaction						
Agglomerate strength is insufficient			√			The material is not sticky enough.
Pneumatic transport						
The material demixes or classifies during transportation		√				—
Solids deposition on pneumatic conveyor walls	√			√		The material is hygroscopic.

scopic nature of a material may be the cause of a deposition problem.

Step 2: determination of target PSD

In this step, we determine the target PSD for a downstream unit under consideration. Table 2 summarizes the relevant design equations for a selected set of downstream units. Using these equations, we can identify the dominant manipulative variables in each unit and, more importantly, determine the necessary changes in PSD to avoid or resolve the problems.

As the equations in Table 2 indicate, cake permeability and porosity are the most important manipulative variables. They are strongly affected by the PSD. Permeability, k, can be estimated from the generalized Blake-Kozeny equation (MacDonald et al., 1991):

$$k = \frac{1}{180}\frac{\epsilon^3}{(1-\epsilon)^2}\left(\frac{M_2}{M_1}\right)^2, \tag{17}$$

where M_1 and M_2 are the first and second moments of the PSD with respect to particle diameter, respectively. The ratio

Table 2. Relevant Equations for Analyzing Crystallization Downstream Processes

Design Equations		References
Filtration		
Filtration time (batch, constant pressure)		Wakeman and Tarleton (1999)
$t_f = \frac{\mu V_f^2}{2kA_f^2\Delta p} + \frac{\mu R_m V_f}{A_f \Delta p}$	(2)	
Filter area (rotary drum filter)		Hill and Ng (1997)
$A_f = 2\pi q_f \left(\frac{M_T \mu}{k(1-\epsilon)\rho_S \psi \omega \Delta p}\right)^{1/2}$	(3)	
Filter area (centrifugal filter)		Zeitsch (1981)
$A_f = \frac{q_f \mu}{k \rho_L \omega^2 \delta} \ln\left(\frac{(r_0+r_1)/2}{(r_0+r_1)/2+\delta}\right)$	(4)	
Washing		
Required wash ratio (single-stage washing)		Wakeman and Tarleton (1999)
$N_w = N_w(N_D, y)$	(5)	
$N_D = \frac{k\Delta p}{\mu\epsilon D_L(1+R_m k/\delta)}$	(6)	
Required wash time		Wakeman (1980)
$t_w = N_w \cdot \frac{\mu\delta^2\epsilon}{k\Delta p}$	(7)	
Recrystallization		
Impurity inclusion level		Chang (1998)
$c_{im} = k_{im}[d_p H(d_p - d_{p,ic})]^m [GH(G-G_{ic})]^n$	(8)	
Deliquoring		
Required deliquoring time (vacuum-drained cake)		Wakeman and Tarleton (1999)
$t_d = c_1 \frac{\mu\epsilon(1-S_\infty)\delta^2}{k\Delta p}\left(\frac{1-S_R}{S_R}\right)^{c_2}$	(9)	
$S_\infty = 0.155(1+0.031 N_{Ca}^{-0.49}); \quad N_{Ca} \geq 10^{-4}$	(10)	
$N_{Ca} = \frac{d_p^2 \epsilon^3 (\rho_L g\delta + \Delta p)}{(1-\epsilon)^2 \sigma\delta}$	(11)	
Required deliquoring time (centrifuged cake)		Wakeman and Tarleton (1999)
$t_d = c_3 \frac{\mu\epsilon(1-S_\infty)}{k\rho_L\omega^2}\left(\frac{1-S_R}{S_R}\right)^{c_4}$	(12)	
$S_\infty = 0.0524\ N_{Ca}^{-0.19}; \quad 10^{-5} \leq N_{Ca} \leq 0.14$	(13a)	
$S_\infty = 0.0139 N_{Ca}^{-0.86}; \ 0.14 \leq N_{Ca} \leq 10$	(13b)	
$N_{Ca} = \frac{d_p^2 \epsilon^3 \rho_L \omega^2 (r_0+r_1)}{2(1-\epsilon)^2 \sigma}$	(14)	
Drying		
Drying time (batch drying)		McCabe et al. (1993)
$t_{\text{dry}} = \frac{W_S}{A_h r_d}\left[(X_0 - X_c) + X_c \ln\frac{X_c}{X_f}\right]$	(15)	
Required heat-transfer area (continuous drying)		—
$A_h = \frac{F_S}{r_d}\left[(X_0 - X) + X_c \ln\frac{X_c}{X_f}\right]$	(16)	

M_2/M_1 is a measure of mean particle size, and will be denoted as d_p throughout this article. The cake porosity, ϵ, mainly depends on the width of the distribution. A wide PSD usually results in a low porosity, since the smaller particles occupy the interstitial space between the large particles. For conceptual design, it is convenient to use two parameters, d_p and ϵ, to represent the PSD.

Next, the role of PSD in the problems associated with each downstream processing unit is discussed in more detail to identify the target PSD.

Solid–liquid separation. Solid–liquid separation, in batch or continuous mode, can be driven by gravity, pressure, vacuum, or centrifugal action. Typical equipment units include the plate and frame filter press (batch), pressure leaf filter (batch), rotary drum filter (continuous), centrifuges and centrifugal filters (batch or continuous), and decanters (batch or continuous). The discussion in this article focuses on the effect of PSD on the performance of filtration units, as they are the most commonly used devices for separating crystals from mother liquor. Similar analyses can be performed for other equipment units as well.

In batch filtration, the key design issue is the required time for filtration. In practice, it is desirable to keep the filtration time reasonably short, for example, below 2 h. As Eq. 2 indicates, the filtration time can be shortened if the permeability of the cake is made higher. From Eq. 17, higher permeability can be achieved by increasing both d_p and ϵ.

In continuous filtration, the design issue is the required filter area to process a given amount of feed. The filter area, A_f, of a rotary vacuum drum filter (Figure 2a) depends strongly on permeability and porosity. By substituting Eq. 17 into Eq. 3, it can be shown that the required filter area is inversely proportional to the mean particle size,

$$A_f \propto \frac{1}{d_p}, \tag{18}$$

and related to the porosity in the following manner,

$$A_f \propto \sqrt{\frac{1-\epsilon}{\epsilon^3}}\,. \tag{19}$$

Since the variation in porosity is seldom drastic, $(1-\epsilon)$ is approximately constant, and $A_f \propto \epsilon^{-3/2}$. In other words, a reduction in filter area can be achieved if particles are made larger and the porosity is increased. For a centrifugal filter (Figure 2b), the dependence of filter area on cake properties is even more pronounced. From Eqs. 4 and 17, A_f is inversely proportional to the mean particle size squared if the porosity stays constant. If the mean particle size remains the same, the filter area is approximately inversely proportional to ϵ^3.

Washing. Washing is normally done in the filter itself. The required wash ratio (N_W), defined as the ratio of the amount of wash liquid used to the amount of liquid originally present in the pores, depends on the dispersion number (N_D) and the desired fraction of the solute remaining in the cake after washing (y). It also depends on the number of stages and circuit configuration (cocurrent or countercurrent) (Chang and Ng, 1998). For example, the equation for single-stage washing is given in Eq. 5. Greater N_D indicates more effective removal, and the same value of y can be achieved with a smaller N_W (Wakeman and Tarleton, 1999). Equation 6 gives the relationship between N_D and the PSD. The wash time, which is the time required for the amount of wash liquor (as specified by the wash ratio) to flow through the filter cake, is given by Eq. 7. Upon inserting Eq. 17 into Eqs. 6 and 7, it is found that the wash ratio and wash time can be reduced by increasing d_p and ϵ.

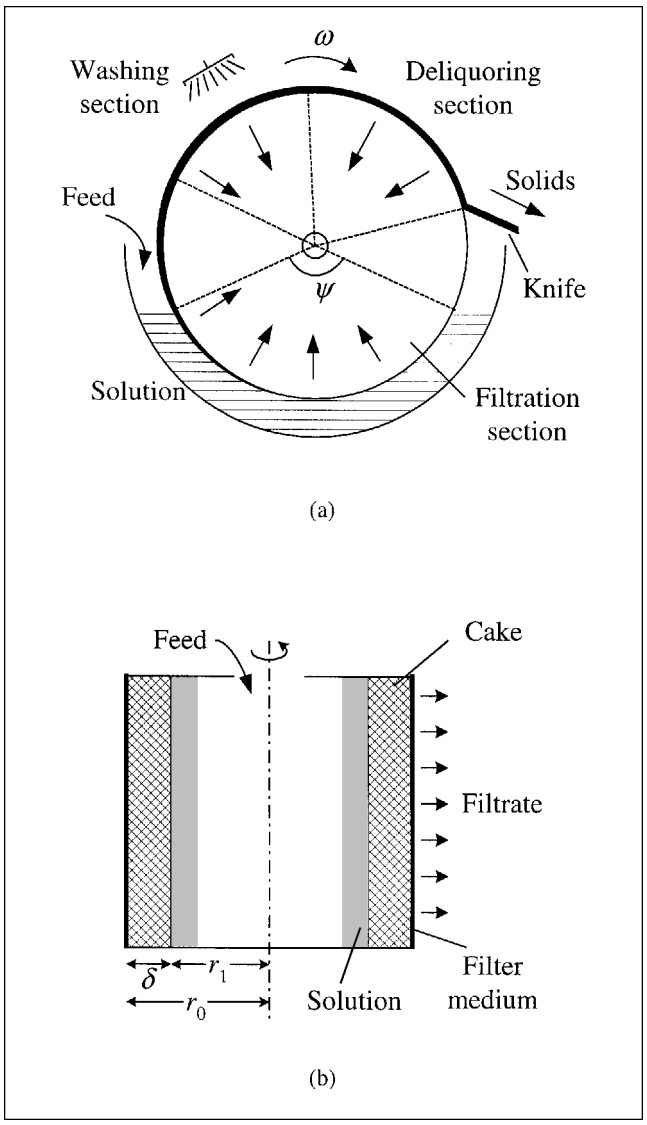

Figure 2. Commonly used filtration equipment units: (a) rotary vacuum drum filter; (b) centrifugal filter.

This, however, is no longer true if the cake thickness changes, as in a rotary drum filter (Figure 2a), where the cake thickness beyond the filtration section depends on the cake porosity and permeability. It can be shown that

$$\delta = \sqrt{\frac{2M_T k \Delta p \psi}{\rho_S \mu (1-\epsilon)\omega}}\,. \tag{20}$$

Substituting into Eq. 7, we obtain

$$t_w = N_w \cdot \frac{2M_T \psi \epsilon}{\rho_S \omega (1-\epsilon)}, \tag{21}$$

which indicates that the wash time is not affected by the mean particle size. This result can also be rationalized as follows. If the production rate is constant, then the volume of cake in the filter, $A_f \delta(1-\epsilon)$, is approximately constant. Furthermore, if the porosity is fixed, $A_f d_p$ is also a constant (Eq. 18), and thus $t_w \propto N_W$ (Eq. 7). In other words, although the cake permeability increases with increasing mean particle size, the cake thickness increases to the same extent. These effects cancel out and the wash time remains the same. On the other hand, increasing the porosity can significantly increase t_w.

Recrystallization. As discussed earlier, minimizing inclusion formation is crucial to avoid a costly recrystallization step. Although various theories have been proposed, the exact mechanism remains elusive. According to the equilibrium adsorption model (Hall, 1953), faster growth rate leads to an increase in impurity inclusions, while the Bruton-Prim-Slichter model (Bruton et al., 1953) predicts the opposite. Experimental data for specific systems were found to agree with the prediction of either of the two models (Botsaris et al., 1967; Mackintosh and White, 1976; Kurihara et al., 1999), although the first model has more support. Furthermore, Denbigh and White (1966) found a critical size below which inclusions are not formed. They also found that when the crystals are larger than the critical size, there is a critical growth rate above which inclusions are formed. This phenomenon was also observed by other researchers (Brooks et al., 1968; Slaminko and Myerson, 1981).

Taking all these factors into account, Eq. 8 can be used to correlate the amount of inclusion under different crystallization conditions. Here, $d_{p,ic}$ is the critical particle size and G_{ic} is the critical growth rate for impurity inclusion. The amount of impurity inclusions can be minimized by keeping the particle size as low as possible, or by adjusting the growth rate as needed. Other methods for preventing inclusions have been proposed (Mullin, 1993), including the addition of certain ionic impurities, increase in the viscosity of the mother liquor, ultrasonic vibration, and change of solvent.

Deliquoring–drying. Deliquoring and drying are linked. The objective is to minimize the overall cycle time of both steps required for reducing the moisture content to a desired level, while at the same time keeping the energy requirement in the dryer as low as possible. The saturation, S, after deliquoring for a period of time is usually expressed as the reduced saturation,

$$S_R = \frac{S - S_\infty}{1 - S_\infty}. \tag{22}$$

Here, S_∞ is the irreducible saturation expressed as the volume fraction of the pores occupied by liquid. It can only be achieved at infinite time. Wakeman (1979) proposed a correlation for the residual saturation as a function of the capillary number, as given in Eq. 10 (for vacuum-drained cakes) and Eq. 13 (for centrifuged cakes). Equations 9 and 12 describe a model for dewatering kinetics (Wakeman and Tarleton, 1999), which leads to an expression for the required time to achieve a desired level of saturation. The constants c_1 to c_4 have different values for different S_R.

After deliquoring, the moisture content is further reduced in the dryer. Equations 15 and 16 give the required drying time for batch drying and the required heat transfer area for continuous drying, respectively. The saturation level can be related to the moisture content X using

$$X = \frac{\rho_L}{\rho_S} \cdot \frac{\epsilon}{1-\epsilon} \cdot S. \tag{23}$$

The higher the saturation level after the deliquoring step, which means shorter deliquoring time, the longer the required drying time to achieve the desired final moisture content. Obviously, there is a trade-off between deliquoring and drying times. From Eqs. 9 to 16, it can be concluded that increasing mean particle size helps to lower the saturation level for a given deliquoring time, or to reduce the required deliquoring time to achieve a given saturation level. The effect of porosity is not as simple. A high porosity leads to a low irreducible saturation and a high permeability. However, it also means that the cake contains more moisture (in kg/kg dry cake) for the same saturation level (Eq. 23). For example, assuming $\rho_S/\rho_L = 0.5$ and $\epsilon = 0.3$, a saturation level of 50% corresponds to a moisture content of 0.107 kg/kg dry cake. But if $\epsilon = 0.4$, the same saturation level corresponds to 0.167 kg liquid/kg dry cake. Therefore, an increase in porosity does not necessarily mean that the saturation after deliquoring or the deliquoring time would decrease.

Step 3: selection of possible means for resolving PSD-related problems

Table 3 summarizes the various means for resolving the problems in crystallization downstream processes. Three types of actions can be taken. We can locally modify the downstream unit where the problem is observed (items A.1–A.4). For example, the rotational speed of a rotary drum filter can be decreased to allow for a longer filtration time. Filter aids can be used to prevent the fines from blocking the filter medium. A hydrocyclone can be installed to remove the fines. However, the impacts of such modifications are usually limited, and installation of new equipment may be unfavorable. Therefore, it is preferable to make design changes on the crystallizer (items B.1–B.5). These modifications alter the PSD in such a way that the related problems can be resolved. The last and most extreme option is to replace the crystallization–filtration train with a spray-drying unit (item C.1), which eliminates the filtration problem. This is a feasible option if the final product is a powder. However, in addition to its high capital and operation costs, spray drying may be unsuitable for some situations (Marshall, 1954; Nonhebel and Moss, 1971). For example, it is not readily usable for toxic products because of the large amount of fines generated. Another drawback is that all impurities in the mother liquor remain in the product.

PSD of a crystallizer product can be modified by controlling nucleation, growth, and crystal agglomeration and break-

Table 3. Possible Ways to Resolve PSD-Related Problems

Modification of the downstream operations
1. Modification of the filtration step
· Reduce rotational speed in continuous filter
· Increase filtration pressure or vacuum level
· Use filter aid to prevent clogging
2. Modification of the washing step
· Increase washing pressure or vacuum level
3. Modification of deliquoring and drying steps
· Increase deliquoring pressure
· Consider using direct instead of indirect heating for drying
· Optimize the deliquoring–drying train
4. Addition of a new unit
· Add a hydrocyclone to remove fines
Modification of the crystallizer operations
1. Control of primary nucleation and crystal growth
(a) Control of global supersaturation
· Operate at a lower supersaturation level
(b) Prevention of high local supersaturation
· Improve mixing in the vessel
· Use better methods of feed introduction
(c) Control of supersaturation profile (batch crystallizers)
· Use controlled cooling, evaporation, or mass separating agent addition
· Use seeding
· Use reheating or partial dissolution
2. Control of secondary nucleation
· Use milder agitation
· Use rounded vessel bottoms
· Improve mixing to have a more uniform suspension of crystals
3. Prevention of particle breakage
· Use milder agitation
4. Modification of crystallizer configurations (continuous crystallizers)
· Use fines removal and/or classified product removal
· Use several crystallizers in stages
5. Minimization of periodic PSD variations (continuous crystallizers)
· Install a surge tank
Modification of the entire separation unit
1. Replacement of the crystallization–filtration train with a spray-drying unit

age rates. Since primary nucleation and crystal growth rates are highly dependent on supersaturation, they can be controlled by manipulating the supersaturation level in the crystallizer. However, operating the crystallizer in a different overall supersaturation level may lead to the need for longer crystallization time or a larger crystallizer. It is well known that spatial homogeneity in large-scale crystallizers is difficult to achieve. The supersaturation tends to be high near the inlet where concentrated solution enters the crystallizer, or in the boiling zone at the top of an evaporative crystallizer. In many cases, the overall process nucleation rate is determined by the maximum local supersaturation instead of by the average value within the vessel. For this reason, controlling local supersaturation is crucial. To improve uniformity in a large crystallizer, a draft tube or multiple impellers can be used (Green, personal communication, 2000). The feed should be fed to a region of high turbulence, such as the immediate vicinity of agitator impellers, in order to ensure rapid mixing. This can be done using dip tubes to place the feed into such regions. Alternatively, the feed can be introduced at a high velocity using nozzles. In batch crystallizers, where the supersaturation changes as the crystallization progresses, the final PSD is determined by the supersaturation profile rather than by the time-averaged value. The control of supersaturation profile is discussed at a later stage.

Secondary nucleation, mainly arising from collision of crystals with the impellers, as well as from fluid shear (Jančić and Grootscholten, 1984), can be minimized if milder agitation is used. Particle breakage can also be reduced this way. Another source of secondary nucleation is the collisions between crystals, which can be minimized if a uniform suspension condition is achieved. Rounded vessel bottoms are used to minimize the formation of recirculating eddies, which may lead to concentration of crystals due to partial settling (Oldshue, 1993). Another alternative to alter the PSD, especially in continuous crystallizers, is by preferentially removing crystals of certain sizes. However, oscillatory behavior of crystallizers can be caused by fines removal, product classification, and secondary nucleation (Randolph et al., 1973). For example, excessive fines removal may lead to insufficient crystal surface area to relieve the supersaturation, such that periodic bursts of nucleation occur (Green, 2000). Stability analyses can be performed to predict such a behavior (Sherwin et al., 1967; Yu and Douglas, 1975). If periodic oscillations cannot be prevented, a surge tank can be installed to minimize the variation.

To some extent, a quantitative analysis can be performed to investigate the effect of various factors on these processes, and therefore on the PSD. However, due to the complexity of crystallization and the hydrodynamics in crystallizers, it is impractical to rely solely on models. For example, an abrupt change of pressure from the reactor to the crystallizer can cause the formation of fines, which do not grow larger. For this reason, qualitative heuristics are used alongside the quantitative analysis in order to come up with a proper strategy to change the PSD. The heuristics are summarized in Table 4. The options for manipulating the crystallizer PSD for batch and continuous crystallizers are now discussed in more detail.

Options for Manipulating PSD in Batch Crystallizers. As mentioned previously, controlling the supersaturation profile is the most common means for controlling the product PSD in a batch crystallizer. The dependence of nucleation and growth rates on supersaturation is often expressed in the power-law form:

$$B = k_b \Delta c^b \tag{24}$$

$$G = k_g \Delta c^g. \tag{25}$$

Both k_b and k_g can be temperature dependent. Due to secondary nucleation, the nucleation rate can also depend on the suspension (magma) density, M_T, and agitation rate, N (Koros et al., 1972; Grootscholten et al., 1982). For such cases, k_b can be written as

$$k_b = k'_b M_T^j N^a. \tag{26}$$

Some systems may exhibit size-dependent growth rate. For such a case, Abegg et al. (1968) proposed

$$k_g = k_{g,0}(1 + k_L L)^l, \tag{27}$$

Table 4. Heuristics for Manipulating PSD in Crystallizers

General heuristics
Consider the use of dip tubes, a nozzle, or multiple feed inlets to improve mixing of the feed into the crystallizer.
Consider using draft tubes to improve mixing in the crystallizer to avoid excessive secondary nucleation, which is especially important in concentrated slurries ($M_T > 100$ kg/m^3) and systems with high specific power input ($\epsilon > 0.5$ W/kg) (Mersmann and Kind, 1988).
If low bulk density of the product is undesirable, consider using spray drying only after experimentally confirming that it can produce solids with the desired bulk density.
Consider using spray drying if the final product should be in the form of fine powder or should readily dissolve in an appropriate solvent.
Do not use spray drying if the mother liquor contains undesirable impurities.
Heuristics for batch crystallizers
Avoid high supersaturation (high N_{Nu}) at the beginning of the batch, if it is desired to obtain large particles and a narrow PSD.
Use an initial supersaturation of about 1–2% of the initial solute concentration (Moore, 1994).
Prefer using an operation mode that gives a supersaturation profile featuring a low Δc at the beginning, followed by a slow increase toward the end of the batch.
Use a seed mass of 0.5–2% of the final product mass to initiate growth in seeded crystallization (Moore, 1994).
The ratio of seed-crystal size to the cubic root of the amount of seeds used to initiate crystallization should remain constant for optimal seeding operation (Jagadesh et al., 1996).
Seeded batch crystallization usually gives larger particles and a more uniform PSD compared to controlled cooling, evaporation, or MSA addition.
The use of partial dissolution is more effective in obtaining narrower PSD and larger average size if larger particles have faster growth rates compared to the small particles, and/or the small particles dissolve much faster than the larger ones.
Heuristics for continuous crystallizers
Irrespective of the means of creating supersaturation (cooling, evaporation, drowning-out, salting-out, reactive), the supersaturation can be lowered by using a larger crystallizer, or a series of crystallizers with an overall higher residence time.
The use of a double drawoff crystallizer or fines dissolution usually increases particle size and minimizes fines in the product (Garside, 1985).
The use of classified product removal generally yields narrower PSD, and thus a higher cake porosity, but does not increase mean particle size (Larson and Randolph, 1969; Garside, 1985).
Multistage operation usually gives larger particle size and narrower PSD (Genck, 1997).
Limit the use of fines dissolution or classified product removal, if it leads to unstable operations yielding periodic variations in PSD.
If a surge tank is to be used for minimizing variation of PSD, consider the fact that steady state in continuous crystallizer is typically achieved after six residence times or greater (Green, personal communication, 2000).

where L represents the crystal size. In reality, crystals having equal dimensions may have different growth rates due to differences in surface characteristics (Genck, 2000). Table 5 lists the typical values of the kinetic parameters involved in crystallization, which can be used as an initial estimate if experimental data were absent. They are based on published crystallization kinetics compiled by Garside and Shah (1980) and Mersmann and Kind (1988), as well as data from various sources (White et al., 1976; Nývlt et al., 1985; Myerson et al., 1986; Mahajan et al., 1991; Genck, 1997).

Table 5. Range of Kinetic Parameter Values and Operating Conditions in Nonreactive Crystallization

k_b	10^4–10^{10}	no/(kg solvent·s)(kg/kg)^b
b	1–3	
k_g	10^{-7}–10^{-3}	(m/s)/(kg/kg)^g
g	0.5–2	
j	0.5–1	
a	1–3	
k_L	0–2	
l	0.5–0.7	
L_0	10^{-9}–10^{-7}	m
Δc	10^{-4}–10^{-2}	kg solute/kg solvent
M_T	10–200	kg/m^3
N	400–2000	rpm
B	10^{-3}–10^{6}	no/(kg solvent·s)
G	10^{-8}–10^{-7}	m/s

To compare the relative importance of nucleation and growth, we define two dimensionless numbers, namely the nucleation number (N_{Nu}) and growth number (N_{Gr}):

$$N_{Nu} = \frac{\text{Nuclei generation rate}}{\text{Supersaturation generation rate}} = \frac{\rho_S k_v L_0^3 B}{d\Delta c/dt} \quad (28)$$

$$N_{Gr} = \frac{\text{Surface integration rate}}{\text{Supersaturation generation rate}} = \frac{\rho_S (3k_v/k_a) a_T G}{d\Delta c/dt}, \quad (29)$$

where L_0 is the nuclei size and a_T is the specific area of the crystals in m^2/kg solvent. In the case of reactive crystallization, the definitions of N_{Nu} and N_{Gr} agree with those defined in Kelkar and Ng (1999). Furthermore, it is convenient to define a parameter

$$\lambda = \frac{N_{Nu}}{N_{Gr}} = \frac{k_a L_0^3 B}{3k_v a_T G}. \quad (30)$$

When N_{Nu} is much higher than N_{Gr} ($\lambda \to \infty$), a large number of small crystals are produced. Furthermore, if the nucleation rate remains high during the course of crystallization, the PSD tends to be broad since new nuclei are generated all the time. On the other hand, if N_{Nu} is much smaller than N_{Gr} ($\lambda \approx 0$), large crystals with narrow PSD can be obtained.

The supersaturation generation rate ($d\Delta c/dt$) depends on the means of achieving supersaturation (Table 6). Table 7 presents commonly used operating modes, which give different profiles of supersaturation with time, for cooling, evaporative, and drowning-out crystallizers. The corresponding profiles of temperature, amount of solvent, amount of mass separating agent (MSA), and supersaturation for these operating policies are depicted in Figure 3. Since B and G both depend on Δc, and normally $b > g$ (Table 5), λ can be kept low by maintaining low supersaturation throughout the course of crystallization.

In natural cooling, the crystallizer is cooled by a cooling medium at a constant temperature. As shown in Figure 3a

Table 6. Expressions for Supersaturation Generation Rate

Crystallizer Type	Method of Supersaturation Generation	Supersaturation Generation Rate
Cooling	Temperature change	$\frac{d\Delta c}{dt} = -\frac{dc^*}{dT}\frac{dT}{dt}$
Evaporative	Isothermal removal of solvent	$\frac{d\Delta c}{dt} = -\frac{c^*}{m_L}\frac{dm_L}{dt}$
Drowning-out	MSA addition	$\frac{d\Delta c}{dt} = -\frac{dc^*}{dm_A}\frac{dm_A}{dt}$
Reactive	Formation of a new chemical species	$\frac{d\Delta c}{dt} = k_r c_f^p$

(curve 1), the temperature decreases exponentially at the beginning of the cooling period, and then slowly approaches the cooling-medium temperature. This results in a very high supersaturation and a high nucleation rate at the beginning (Figure 3d). Controlled cooling at a constant rate (curve 2) also features a peak in supersaturation. Similar supersaturation profiles are obtained with constant evaporation rate (curve 5) in evaporative crystallizers and constant MSA addition rate (curve 8) in drowning-out crystallizers. To obtain larger crystals with narrower PSD, the supersaturation has to be kept low. Jones and Mullin (1974) proposed that operation at constant supersaturation leads to a reduction in the amount of nuclei formed, and thus to the production of large crystals. Mathematical models for obtaining temperature profiles that give rise to constant supersaturation operation are available (Eqs. 33 and 34). The profiles (curves 3 and 4) feature a slow temperature drop at the beginning followed by increasing cooling rate toward the end of the batch (Figure 3a). This is possible because as crystals grow larger, a larger area is available for growth. Similar models for evaporative and drowning-out crystallizers are given by Eqs. 36, 37 and 39.

Efforts toward optimization of batch crystallization operation modes have also been made. For example, Lang et al. (1999) applied dynamic optimization techniques to obtain the temperature profile giving maximum crystal size and minimum batch time. However, it must be realized that accurate knowledge of crystallization kinetics is critical in such efforts.

Seeding can have an even more pronounced effect on product PSD (Chianese et al., 1984; Bohlin and Rasmuson, 1992). If the crystallizer is operated under a condition where nucleation is negligible, the amount and PSD of crystal seeds introduced to the crystallizer play a decisive role in determining the product PSD. Jagadesh et al. (1996, 1999) found that large crystals could be obtained even with natural cooling mode, by using an appropriate seed concentration. Chung et al. (1999) reported that changing the seed mass could have an order-of-magnitude effect on product mean particle size, and an even more significant effect on the width of distribution. This is clearly reflected in the expression of λ in Eq. 30.

Table 7. Examples of Crystallizer Operation Policies

Crystallizer Type and Operation Modes	Model		Key Assumptions/Objectives
Cooling			
1. Natural cooling	$\frac{dT}{dt} = -\frac{UA_h}{mC_p}(T - T_m)$	(31)	Constant cooling-medium temperature
2. Constant cooling rate	$\frac{dT}{dt} = k_c$	(32)	—
3. Programmed cooling with seeding (Mullin and Nývlt, 1971)	$\frac{dT}{dt} = -\frac{3m_s G}{L_s m_L (dc^*/dT)}\left(1 + \frac{Gt}{L_s}\right)^2$	(33)	Constant supersaturation Size-independent growth rate Negligible nucleation
4. Programmed cooling (Tavare, 1995)	$\frac{dT}{dt} = \frac{k_v \rho_s G^3 B t^3}{dc^*/dT}$	(34)	Constant supersaturation Size-independent growth rate No seeding
Evaporative			
5. Constant evaporation rate	$\frac{dm_L}{dt} = k_e$	(35)	—
6. Programmed evaporation with seeding (Larson and Garside, 1973)	$\frac{dm_L}{dt} = \frac{3m_s G}{L_s c^*}\left(1 + \frac{Gt}{L_s}\right)^2$	(36)	Constant supersaturation Size-independent growth rate Negligible nucleation
7. Programmed evaporation (Tavare, 1995)	$\frac{d^4 m_L}{dt^4} = -6k_v \rho_S G^3 B m_L$	(37)	Constant supersaturation Size-independent growth rate No seeding
Drowning-out			
8. Constant MSA addition rate	$\frac{dm_A}{dt} = k_d$	(38)	—
9. Programmed MSA addition (Tavare, 1995)	$\frac{dm_A}{dt} = -\frac{k_v \rho_S G^3 B t^3}{dc^*/dm_A}$	(39)	Constant supersaturation Size-independent growth rate No seeding

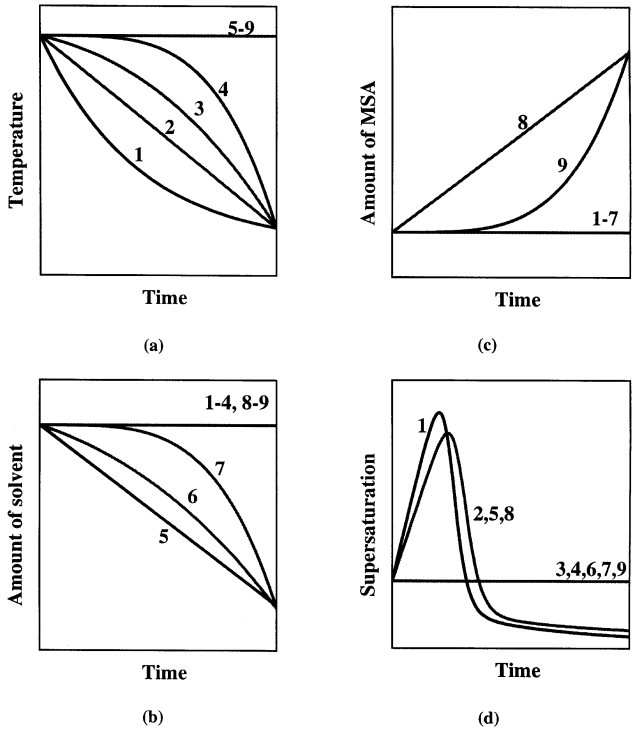

Figure 3. Typical profiles in batch crystallizers: (a) temperature; (b) amount of solvent; (c) amount of MSA; (d) supersaturation.

Both the mass and PSD of the seed determines the specific crystal area, a_T. A high value of a_T causes λ to be low right from the beginning of the crystallization, which leads to negligible nucleation. Seeding also has other benefits, such as controlling the polymorphic form being crystallized (McCrone, 1965).

Another alternative is to remove small crystals from the crystal population in the crystallizer. This can be done either by selectively removing small particles using a classifying device (Jones et al., 1984), or by introducing periods with negative supersaturation such that dissolution occurs (Heffels et al., 1991). For cooling crystallizers, the idea of partial dissolution can be generalized to include reheating, where the temperature is increased in the middle of the crystallization cycle, causing a drop in supersaturation. If the supersaturation becomes negative, then dissolution occurs. But even if it still has a positive value, λ would decrease significantly, thus promoting the formation of larger particles. Partial dissolution has also been reported to eliminate encrustation in the crystallizer (Heffels et al., 1991).

Options for Manipulating PSD in Continuous Crystallizers. In continuous crystallizers, PSD can be manipulated by considering different process configurations utilizing peripheral devices such as partial dissolvers and particle classifiers. Classification can be performed with external devices such as hydrocyclones, elutriators, or lamella settlers, or using an internal device, such as the annular settling zone, in a draft-tube baffled (DTB) crystallizer (Green, personal communication, 2000).

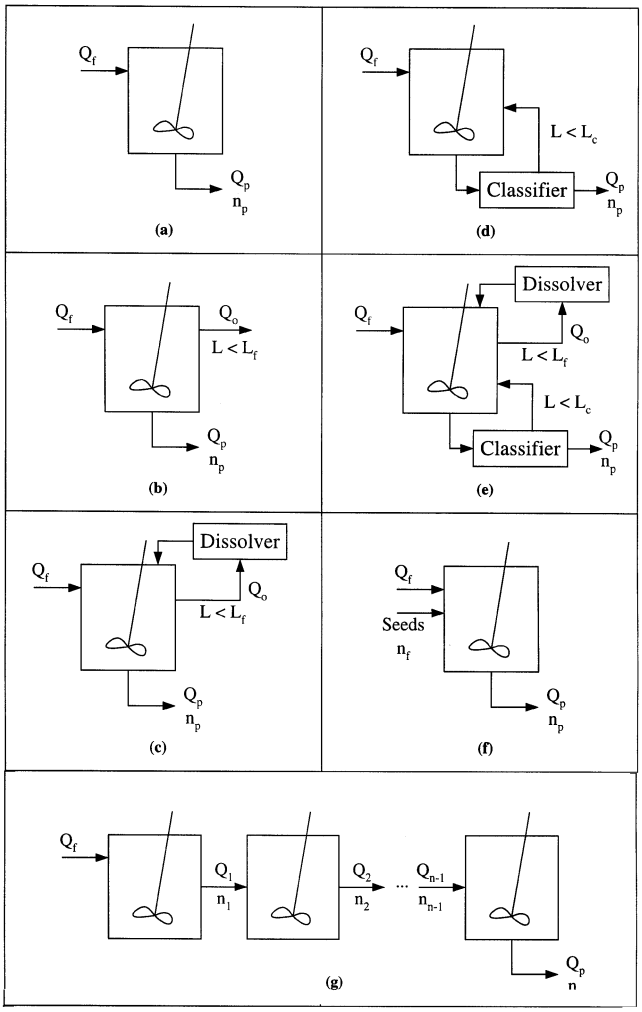

Figure 4. Continuous crystallizer configurations: (a) MSMPR; (b) with fines removal; (c) with fines dissolution; (d) with classified product removal; (e) with fines dissolution and classified product removal; (f) with seed crystals in the feed; (g) multistage crsytallizers.

Figure 4 depicts the major configuration options. The mixed-suspension mixed-product removal (MSMPR) crystallizer (Figure 4a) serves as the reference. Figure 4b shows a crystallizer with fines removal, which is also referred to as a double drawoff (DDO) or clear-liquor advance crystallizer. As in batch operation, uncontrolled nucleation, which leads to small particle size, can be minimized with a smaller supersaturation. By continuously removing the fines, the growth rate will benefit the larger particles more, and result in larger particles. Alternatively, fines can be dissolved in a dissolver and recycled back to the crystallizer (Figure 4c). Since most of fines are removed or destroyed, the fines fraction in the product stream will decrease. Figure 4d is a representation of a classified product removal crystallizer. Larger particles are preferentially removed from the crystallizer, while smaller particles are recycled. The crystal-size distribution is usually much narrower than that of an MSMPR crystallizer. How-

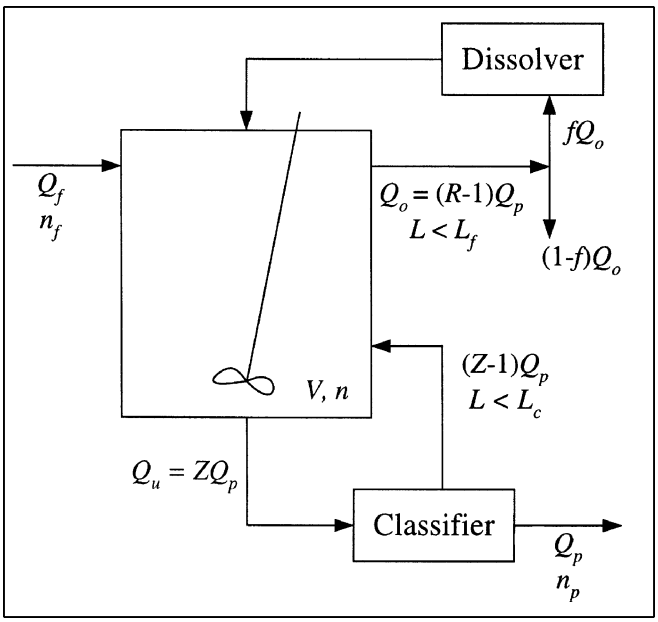

Figure 5. Generic crystallizer model.

ever, this may be accompanied by a decrease in average crystal-size, if the production rate is kept constant (Larson and Randolph, 1969). Figure 4e depicts a combination of fines dissolution and classified product removal. Seeded crystallizer (Figure 4f) is another option to improve the crystal-size distribution.

Other alternatives can be obtained by combining these basic units. For example, a multistage crystallizer (Figure 4g) is quite common in industrial practice, due to advantages such as lower energy consumption (Liu et al., 1991). In principle, narrower PSD can be achieved as the number of crystallizers is increased. This is because a gradual drop in supersaturation can be achieved by operating each crystallizer at a different temperature or pressure. However, preventing appreciable nucleation in the second and subsequent crystallizers, which is critical to the success of such narrowing, is difficult to achieve in practice (Garside, 1985).

Step 4: evaluation of alternatives

After identifying the alternative suitable operation modes, we need to compare them on the basis of performance. For a continuous crystallizer, a generic steady-state crystallizer model is developed (Figure 5). It consists of a well-mixed crystallizer and devices for fines removal, fines destruction, and classified product removal. This generic model, similar to the $R-Z$ model (Larson and Randolph, 1969), is as follows:

$$V\frac{d(Gn)}{dL} + ZQ_p n + (R-1)Q_p n\left[1 - H(L - L_f)\right] = Q_f n_f + (Z-1)Q_p n\left[1 - H(L - L_c)\right], \quad (40)$$

where G is the crystal growth rate, n is the population density (number of crystals per unit size per unit volume) in the crystallizer, and H is the Heaviside function. The first term represents crystal growth, while the second and third terms represent product removal and fines removal, respectively. The remaining two terms represent feed stream and recycle stream from the product classifier, respectively. Only particles smaller than L_f can be removed by the fines removal stream. When clear liquid is discharged in the overflow, $L_f = 0$. The flow to the classifier is Z times of the product flow. Only particles smaller than L_c are recycled back to crystallizer from the product classifier. The parameter f, which distinguishes fines dissolution ($f = 1$) from DDO crystallizer ($f = 0$), does not affect the population balance. For a well-mixed batch crystallizer, the model becomes

$$\frac{\partial n}{\partial t} + \frac{\partial (Gn)}{\partial L} = 0. \quad (41)$$

To evaluate the impact of the resulting PSD on downstream processing units, the models described in Table 2 are used. The cake porosity can be estimated from the PSD using a correlation developed by Ouchiyama and Tanaka (1984):

$$\epsilon = 1 - \frac{\sum_{i=1}^{m} D_i^3 f_i}{\sum_{i=1}^{m} (D_i - \langle D\rangle)^3 H(D_i - \langle D\rangle) f_i + \frac{1}{\bar{n}} \sum_{i=1}^{m} \left[(D_i + \langle D\rangle)^3 - (D_i - \langle D\rangle)^3 H(D_i - \langle D\rangle)\right] f_i}, \quad (42)$$

where

$$\bar{n} = 1 + \frac{4(7 - 8\bar{\epsilon}_0)\langle D\rangle}{13} \frac{\sum_{i=1}^{m} (D_i + \langle D\rangle)^2 \left(1 - \frac{3}{8}\frac{\langle D\rangle}{D_i + \langle D\rangle}\right) f_i}{\sum_{i=1}^{m} \left[D_i^3 - (D_i - \langle D\rangle)^3 H(D_i - \langle D\rangle)\right] f_i}. \quad (43)$$

In these equations, f_i is the number fraction of particles in interval i; $\bar{\epsilon}_0$ is the average porosity of uniformly sized spheres; and $\langle D \rangle$ is the mean particle diameter. The accuracy of the model drops drastically if the number of intervals, m, is large (Hill and Ng, 1997), but nonetheless it gives the correct trend. Other models for predicting PSD are available, but are significantly more complicated. For example, Rouault and Assouline (1998) proposed a probabilistic approach to find the pore-size distribution, which predicts not only the porosity but also the interconnectivity between the pores. The design procedure is now illustrated using two examples.

Examples

Example 1: batch crystallization of a specialty chemical

Batch crystallization is widely used to recover specialty chemicals from their reaction mixtures. Let us consider a situation where a company has decided to switch to a slightly different chemical formula of an existing specialty chemical product, which has a higher market potential. Since the new product is essentially the same as the current one, the plan is to carry out the production in the existing plant. The batch-cooling crystallizer has a 5-tonne capacity, producing 400 kg (dry basis) of the new product per batch. The crystals are filtered and washed in a plate-and-frame filter press operating at a constant pressure. The cake is then deliquored with pressurized air, and finally dried in a batch tray dryer. In a trial run, it is found that filtration at maximum pressure took about 3 h to finish, which is considered unacceptable. Process modifications are needed to reduce the filtration time to less than 2 h. Relevant input information is provided in Table 8. Perfect mixing is assumed in the crystallizer.

Step 1. From Table 1, long filtration time is likely to be a result of low permeability and porosity, which is in turn caused by small particle size and wide PSD. Indeed, analysis reveals that the crystals from the trial production have a mean particle size of 23.8 μm and a porosity of 0.376. Washing is not likely to be a concern, since N_D is very high (Eq. 6), leading to a minimum washing liquid requirement. The wash time (Eq. 7) is also very short, on the order of 2 to 3 min. With a deliquoring time of 10 min, the moisture content in the filter cake is reduced to about 10% (Eq. 9), and a drying time of about 30 min is necessary to further reduce the moisture content to the desired level of 1% (dry solids basis) (Eq. 15).

Step 2. The mean particle size and porosity should be increased to reduce the filtration time. Since increasing porosity may increase deliquoring and drying times (Eqs. 9 and 15), we want to consider the total cycle time, that is, the time

Table 8. Input Information for Example 1

Physical properties and kinetics data	
Crystal density	2,250 $kg \cdot m^{-3}$
Solution density	1,100 $kg \cdot m^{-3}$
Solution viscosity	0.0011 $kg \cdot m^{-1} \cdot s^{-1}$
Solution surface tension	0.07 $N \cdot m^{-1}$
Crystal-shape factors	$k_v = 0.5325$
	$k_a = 3.5$
Solubility of specialty chemical	$a = 0.0027$
$S = aT + b$ (kg/kg)	$b = 0.085$
Growth rate	$k_g = 1.02 \times 10^{-6}$ (m/s)/(kg/kg)^g
	$g = 1.0$
Nucleation rate ($no \cdot m^{-3} \cdot s^{-1}$)	$k_R = 8 \times 10^{38}$ [no/s/m^3/(m/s)^i/(kg/kg)^j]
$B = k_R G^i M_T^j$	$i = 4.0$
	$j = 0.2$
Inclusion formation (kg impurity/kg dry solids)	$k_i = 6.4 \times 10^{23}$
$c_{im} = k_{im}[d_p H(d_p - d_{p,ic})]^m [GH(G - G_{ic})]^n$	$m = 1.5$
	$n = 3.0$
	$d_{p,ic} = 5$ μm
	$G_{ic} = 10^{-8}$ m/s
Feed and product specifications	
Feed temperature	100°C
Feed composition	0.35 kg product/kg H_2O
Product impurity level (dry basis)	50 μg/g
Product moisture content	0.01 kg H_2O/kg dry solids
Batch crystallizer	
Crystallizer final temperature	50°C
Heat-transfer coefficient (for natural cooling)	0.001 s^{-1}
Plate and frame pressure filter	
Total filter area	2.4 m^2
Medium resistance	10^9 m^{-1}
Wash ratio	2
Filtration-washing pressure	300 $kN \cdot m^{-2}$
Deliquoring pressure	400 $kN \cdot m^{-2}$
Tray dryer	
Drying rate	0.027 $kg \cdot m^{-2} \cdot s^{-1}$
Critical moisture content	0.015 kg H_2O/kg dry solids
Available heat-transfer area	8 m^2

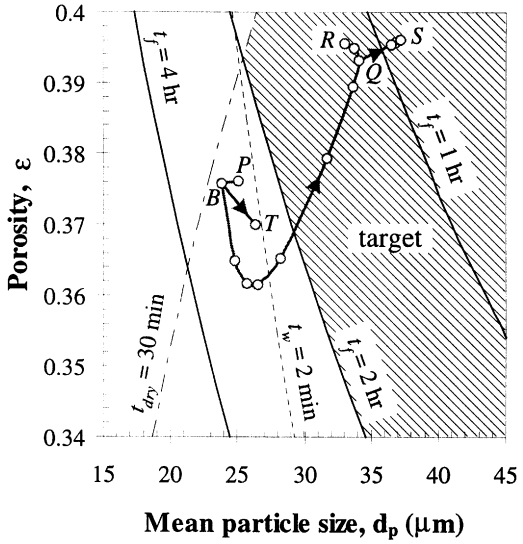

Figure 6. Simulation results for Example 1 in a d_p-ϵ diagram.

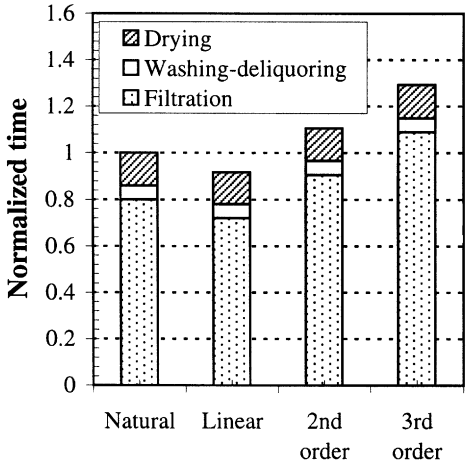

(a)

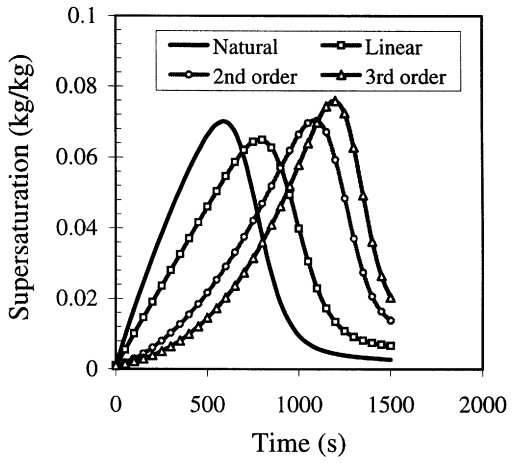

(b)

Figure 7. Dependence on order of cooling (Example 1) of (a) normalized cycle times at constant deliquoring time; (b) supersaturation profiles.

required for filtration–washing–deliquoring–drying, rather than the filtration time alone. Two processing options are considered to illustrate the system performance. First, the deliquoring time is kept constant at 10 min, while the drying time is to be minimized. Second, the moisture content of the cake entering the dryer is assumed to be constant at 10% (corresponding to a drying time of 29.3 min), while the deliquoring time is to be minimized. Furthermore, we also want to track the impurity level in the product, as well as the fines content. The latter is important because a high fines content may lead to filter-medium clogging.

Step 3. The trial run is performed under natural cooling with no seeding. This is taken as the base case. As suggested by Table 3, we consider the options of using controlled cooling, seeding, and dissolution to increase the particle size and porosity. According to a heuristic in Table 4, we use about 0.001 kg seeds/kg solvent as a starting point, that is, about 1% of the final product mass.

Step 4. Let us begin with the first case, where the deliquoring time is constant. To evaluate the effect of changing conditions, we present the calculation results in a $d_p - \epsilon$ diagram (Figure 6). Each point on the diagram represents the particle size and porosity of a crystallization product. Equation 2 is used to calculate the filtration time, and the result is shown as the solid contour lines on the diagram. Washing and drying times are calculated using Eqs. 7 and 15, respectively. The dotted line represents the locus of points with a constant washing time, and the dashed line refers to points with a constant drying time. The base case is represented by point B in the figure.

The effect of controlled cooling is shown by path BP (Figure 6). We define the order of cooling as the power x in the equation

$$\frac{T - T_0}{T_f - T_0} = \left(\frac{t}{t_f}\right)^x, \tag{44}$$

where the subscripts 0 and f represent initial and final conditions, respectively. With linear cooling ($x = 1$), a reduction of filtration time to about 2.5 h can be achieved (point P). However, further increase in x causes the mean size and porosity to decrease. This is not drawn in Figure 6 to maintain the clarity of the figure. As shown in Figure 7a, second- and third-order cooling give even higher cycle time than the base case. The variation in d_p and ϵ can be understood by looking at the change in supersaturation with time (Figure 7). Compared to the base case (natural cooling), controlled cooling features a less sharp rise in supersaturation. As x increases, the peak is shifted to a later time. When $x > 1$, the crystallization starts with very slow nucleation and growth, such that the supersaturation builds up and bursts of nuclei are generated toward the end due to the high supersaturation.

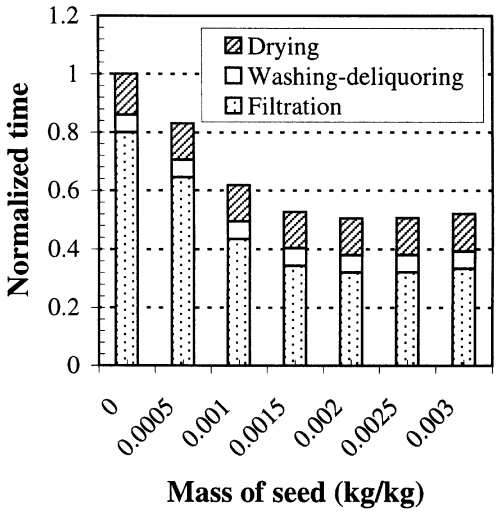

Figure 8. Dependence of normalized cycle times at constant deliquoring time on amount of seed (Example 1).

As discussed previously, seeding can be used to improve PSD. Path *BQR* in Figure 6 shows the change in d_p and ϵ with an increasing mass of seeds under natural cooling. The seeds are assumed to have a nearly uniform PSD with a mean particle size of 10 μm. With the addition of a small amount of seeds, the porosity tends to decrease while mean size increases. This indicates that many small particles are formed due to an insufficient amount of seeds to suppress nucleation. A further increase in seed mass leads to an increase in both d_p and ϵ. Using 0.002 kg of seeds per kg solvent (about 2% of the final product mass), a mean particle size of 34.1 μm and a porosity of 0.393 (point *Q*) can be achieved. This corresponds to a filtration time of about 67 min, and a drying time of about 26 min. As shown in Figure 8, the total cycle time is reduced by almost 50% as compared to the base case. However, if the seed mass is further increased to 0.003 kg/kg (point *R*), the product size decreases, although a further increase in porosity is observed. The filtration time increases, and so does the total cycle time (Figure 8). This is because the deposited material must be distributed among a greater number of seed crystals, thus yielding a greater number of uniform but smaller particles.

Combination of controlled cooling and seeding is proven to give the best results, as shown by Path *QS* in Figure 6. Using 0.002 kg seed/kg solvent, second-order cooling improves the particle size to 37.2 μm and the porosity to 0.396 (point *S*). The filtration time decreases to less than 1 h, and the drying time is about 25 min. The total cycle time is reduced by 56% compared to the base case (Figure 9a). Figure 9b shows a comparison of the supersaturation profiles of different crystallization modes. The addition of seeds results in a significant decrease in the maximum supersaturation. The supersaturation is further reduced by combining seeding with controlled cooling.

Path *BT* shows the change in d_p and ϵ due to reheating (Figure 6). Point *T* represents the outcome when the solution is reheated using steam at 100°C in the heat exchanger for 200 s, after crystallization with natural cooling has progressed

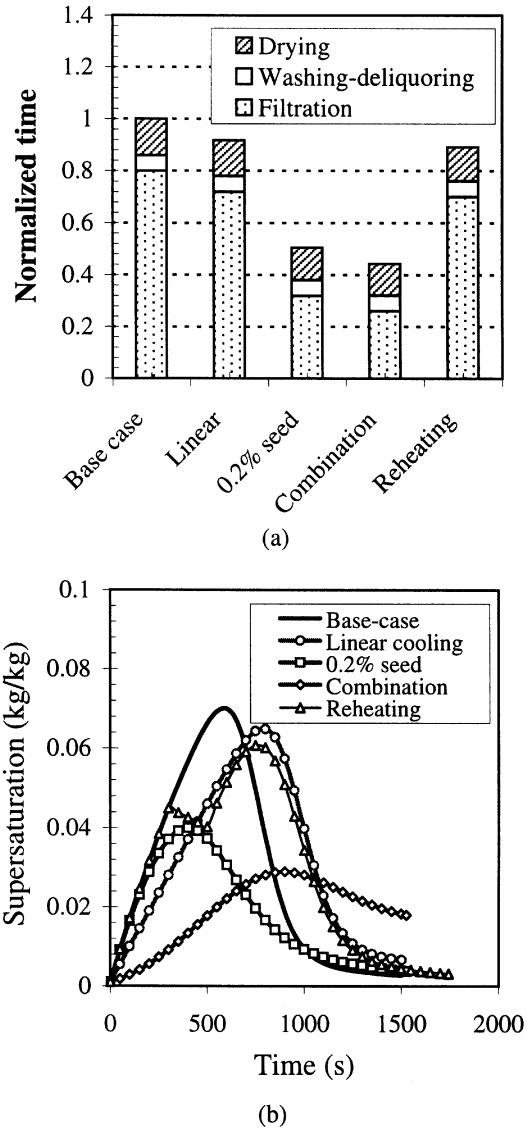

Figure 9. Dependence on operating mode (Example 1) of (a) normalized cycle times at constant deliquoring time; (b) supersaturation profiles.

for about 300 s. As depicted in Figure 9b, this causes a drop in the supersaturation. Another increase in supersaturation occurs after the cooling is resumed, but the peak is now lower than that of the base case. The resulting mean particle size is 26.3 μm, and the porosity decreases to 0.370. The total cycle time decreases by about 11% compared to the base-case value (Figure 9a), which is not as attractive as the combined seeding and controlled-cooling case. It should also be noted that because of reheating, the crystallization time is prolonged from 25 min to 28 min. Clearly, there is a trade-off between crystallization time and filtration–deliquoring–drying times.

The effect of different operating modes on fines content and inclusion impurity level is shown in Figure 10. Paths *BP*, *BQR*, and *BT* indicate the change in fines content and impurity level due to controlled cooling, seeding, and reheating, respectively. Path *QS* indicates the effect of controlled cool-

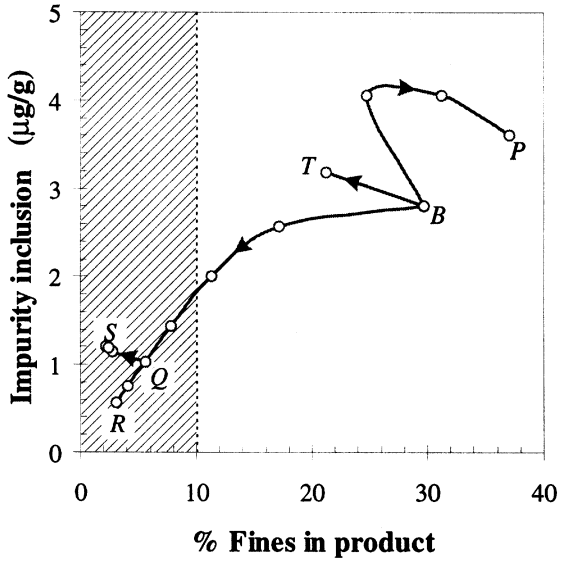

Figure 10. Effect of different operating modes on the amount of fines and impurity inclusion in the product (Example 1).

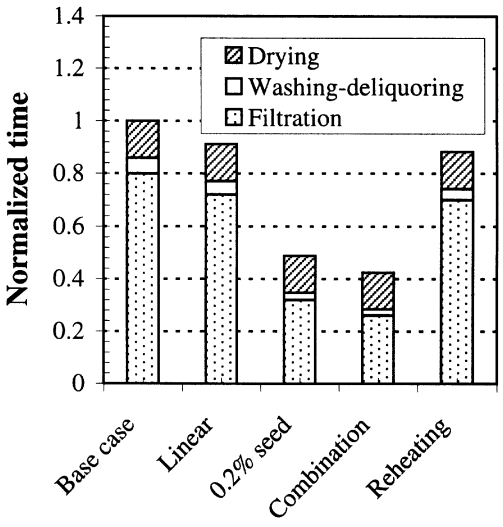

Figure 11. Dependence of normalized cycle times at constant drying time on operating mode (Example 1).

ing using 0.002 kg seed/kg solvent. If we set a target that the amount of fines (defined here as particles smaller than 20 μm) should not exceed 10%, seeding is the only way to achieve the target. Using combined seeding and controlled cooling, the fines content can be reduced to about 3% (point *S*). Simulation results also show that the inclusion impurity level ranges between 0.5 and 4 μg/g, which is far below the acceptable level of 50 μg/g. This is mostly because the average growth rate of the crystals is only slightly above the critical growth rate for impurity inclusions, which is 10^{-8} m/s for this product (Table 8).

A similar analysis can be performed for the case where the drying operation is fixed. The results are summarized in Figure 11. The use of linear cooling leads to about a 9% decrease in total cycle time, while seeding using 0.002 kg seed/kg solvent leads to an almost 51% decrease. Combined seeding and controlled cooling can further reduce the total cycle time to less than an hour, or only 42.5% of the base-case value. It is therefore evident that for this example, the effect of PSD on deliquoring time is slightly greater than its effect on drying time. Further analysis can be performed to find an optimum cycle time, but it will not be pursued here.

Example 2: production of adipic acid

Adipic acid is an important dicarboxylic acid produced commercially from cyclohexane using a two-step oxidation process (Kroschwitz and Howe-Grant, 1991). The product is recovered by crystallization. During oxidation, two dibasic acids, glutaric and succinic acids, are also formed as the major impurity byproducts. In this example, we consider a continuous process for producing 25,000 kg/h (6.94 kg/s) of adipic acid (dry basis). The crystals are filtered, washed, and deliquored in a rotary drum filter, and dried in a continuous rotary dryer. The input information is presented in Table 9. In continuous crystallizers, there exist regions of high supersaturation with high nucleation rate. To take this into account in the simulations, we use an effective nucleation rate, which has a larger value than that for uniform mixing.

Step 1. We first consider an MSMPR crystallizer with a supersaturation of about 0.005 kg/kg, corresponding to a growth rate of 4.8×10^{-8} m/s. As a base case, we assume an effective nucleation rate of $4\times10^{9}/\mathrm{m}^3\cdot\mathrm{s}$, that is about 5 times larger than the nucleation rate predicted from kinetics. Under this condition, the predicted mean particle size is 48.8 μm and the porosity is 0.296. The required filter area is about 39 m^2. Since the largest available unit has an area of about 30 m^2, parallel units must be used. A more attractive option is reducing the filter area to below 30 m^2. To prevent filter-medium clogging, we try to limit the amount of fines to below 4%.

Step 2. To reduce the filter area, larger particle size and porosity would be required. Since a rotary-drum filter is used, washing and deliquoring times are fixed by the rotational speed of the drum. To minimize the residual moisture content after deliquoring, the porosity should be kept as low as possible. It is desirable that the moisture content of the dryer feed be less than 15%.

Step 3. There are several ways to increase the particle size and porosity in continuous crystallizers: using fines dissolution, classified product removal, and combinations of them. We can also try to improve mixing to decrease the effective nucleation rate (Table 3).

Step 4. Figure 12 shows the calculation results. Each solid curve represents constant filter area for different combinations of porosity and mean particle size (Eq. 3). The effective nucleation rate is assumed to be constant and the crystallizer volume is kept at 29.1 m^3. The base case is denoted by point *B*, and the shaded area represents the target. The effect of fines dissolution is shown by path *BP*. As *R* increases, the mean particle size increases, but the porosity goes down. There is an insignificant reduction in filter area. Classified product removal increases porosity but hardly affects mean

Table 9. Input Information for Example 2

Physical properties and kinetics data	
Crystal density of adipic acid	1,360 $kg \cdot m^{-3}$
Solution density	1,300 $kg \cdot m^{-3}$
Solution viscosity	0.0011 $kg \cdot m^{-1} \cdot s^{-1}$
Solution surface tension	0.07 $N \cdot m^{-1}$
Crystal-shape factors	$k_v = 0.5325$
	$k_a = 3.5$
Solubility of adipic acid	$a = 0.00575$
$S = aT + b$(kg/kg)	$b = -0.1775$
Growth rate (Liu et al., 1991)	$k_g = 1.99 \times 10^{-5}$ (m/s)/(kg/kg)^g
	$g = 1.2$
Nucleation rate (no $\cdot m^{-3} \cdot s^{-1}$)(Liu et al., 1991)	$k_R = 9.11 \times 10^{32}$ (no/s/m^3/(m/s)^i/(kg/kg)^j)
$B = k_R G^i M_T^j$	$i = 3.5$
	$j = 0.4$
Inclusion formation (kg impurity/kg AA)	$k_i = 9.1 \times 10^{22}$
$c_{im} = k_{im}[(d_p H(d_p - d_{p,ic})]^m [GH(G - G_{ic})]^n$	$m = 1.5$
	$n = 3.0$
	$d_{p,ic} = 50$ μm
	$G_{ic} = 3.33 \times 10^{-8}$ m/s
Feed and product specifications	
Feed temperature	70°C
Feed composition	0.225 kg AA/kg H_2O
Product impurity level (dry basis)	150 μg/g
Product moisture content	0.01 kg H_2O/kg dry solids
Continuous MSMPR crystallizer	
Crystallizer temperature	50°C
Rotary-drum vacuum filter	
Rotational speed	1 rpm = 0.105 $rad \cdot s^{-1}$
Angle of submergence	135°
Medium resistance	10^9 m^{-1}
Vacuum level for filtration and washing	26,000 $N \cdot m^{-2}$
Portion for washing	0.2
Wash ratio	1.75
Portion for deliquoring	0.3
Pressure level for washing	65,000 $N \cdot m^{-2}$
Rotary dryer	
Superficial air velocity	1.5 $m \cdot s^{-1}$
Logarithmic mean temperature difference	74.5°C
Solids fractional filling	0.15

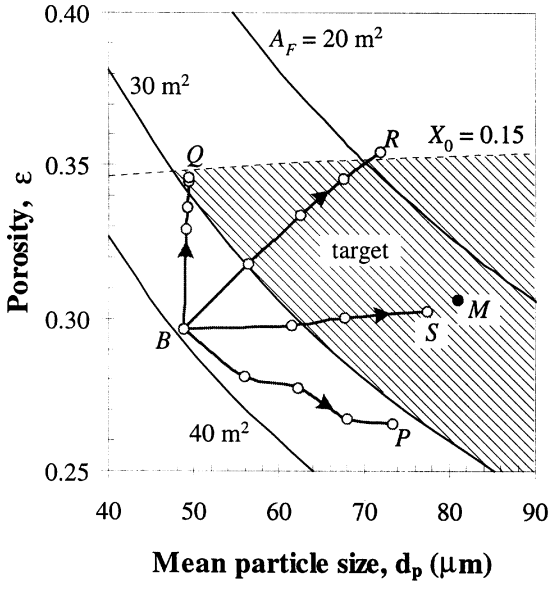

Figure 12. Simulation results for Example 2 in a d_p-ϵ diagram.

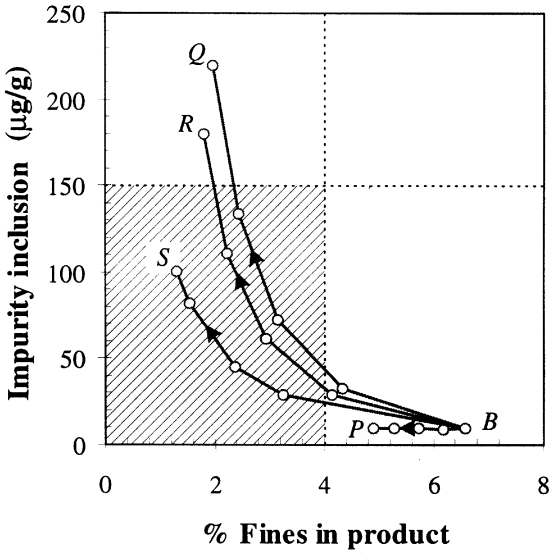

Figure 13. Effect of different crystallizer configurations on the amount of fines and impurity inclusion in the product (Example 2).

particle size, as shown by path BQ. At $Z = 2.5$ the target is achieved, and further increase in Z does not give significant improvement. Path BR shows the effect of using fines dissolution combined with classified product removal, with $R = Z$. Both porosity and mean particle size increase, and the target filter area is achieved when $R > 1.5$. However, when $R = Z = 3$, the porosity becomes so high that deliquoring with the available time (18 s) cannot reduce the moisture content to 15%. The effect of improved mixing, as represented by decreasing effective nucleation rate, is shown by path BS. As the effective nucleation rate decreases, the mean particle size increases, but the porosity does not change by much. Point M represents the perfect mixing (MSMPR) condition. Clearly, we can also combine improved mixing, fines dissolution, and classified product removal.

We also need to consider the amount of fines and impurity inclusion. As Figure 13 shows, changing R (path BP) from 1 to 3 does reduce the amount of fines to about 5%, which is still too high. Increasing Z (path BQ) or both R and Z (path BR) has the effect of decreasing the amount of fines, but at the same time increasing the impurity level. This is mainly because of a faster growth rate in the crystallizer. When Z is increased above 2.5, the impurity level would exceed the allowable limit of 150 μg/g (point Q). Improving mixing (path BS) seems to be the best strategy to reduce the amount of fines while keeping the impurity level within the acceptable limits.

Conclusions

Despite the extensive research activities in the area of crystallization and solid–liquid separations, few attempts have been made to integrate the two interconnected processes. This is a serious omission because many operational problems in crystallization processes can be ameliorated or eliminated by considering the crystallizer and downstream units as an integrated system.

As an effort to fill this gap, we have developed a four-step procedure for the design of an integrated crystallization system. Problems in the crystallization downstream unit operations such as filtration, washing, deliquoring, and drying are identified. These problems are resolved by changing the crystallizer and its operations or the operating conditions of a downstream equipment unit and by installing additional devices. The process alternatives thus generated are evaluated to identify the best candidate for a new plant design or a retrofit.

While this approach for the design of an integrated crystallization system is general in nature, it is not expected to cover all problems encountered in practice. For example, we do not consider fibrous materials, for which some of the models discussed in this article are no longer valid. Also, because only simplified models are considered, the predicted process performance is not exact. Nonetheless, the procedure can be expected to point to the right direction for necessary action, identify the need for more accurate experimental data, and provide a base case for rigorous optimization. It should be noted that such rigorous optimization relies heavily on the availability of appropriate models for PSD predictions. Provided that such models are available, one can formulate a superstructure that embeds all possible crystallizer configurations, and use it to find an optimal solution. The simplest example of such a superstructure is the generic continuous crystallizer model depicted in Figure 5.

A similar approach has been taken to systematically resolve operational problems in bulk solids processing plants (Wibowo and Ng, 2001). Since crystals are often fed into a bulk solids processing plant to produce a solids product, it is desirable to consider the interactions among crystallization, downstream processing, and bulk-solids processing systems. Efforts in this direction are now in progress.

Acknowledgment

The support from the National Science Foundation (Grant No. CTS-9908667) for this work is gratefully acknowledged.

Notation

a = order of nucleation rate constant with respect to agitation rate, dimensionless
a_T = specific area of crystals, $m^2 \cdot (kg\ solvent)^{-1}$
A_f = filter area, m^2
A_h = area available for heat transfer, m^2
b = order of nucleation rate with respect to supersaturation, dimensionless
B = nucleation rate, $no \cdot (kg\ solvent)^{-1} \cdot s^{-1}$
c = solution concentration, $kg \cdot (kg\ solvent)^{-1}$
c^* = solubility, $kg \cdot (kg\ solvent)^{-1}$
$\Delta c = c - c^*$ = supersaturation, $kg \cdot (kg\ solvent)^{-1}$
c_1, c_2, c_3, c_4 = constants (in Eqs. 9 and 12), dimensionless
c_f = concentration of reactant in feed, $kg \cdot (kg\ solvent)^{-1}$
c_{im} = concentration of enclosed impurity, $kg \cdot (kg\ solid)^{-1}$
d_p, $\langle D \rangle$ = mean particle size, m
$d_{p,ic}$ = critical particle size for impurity inclusion, m
D_i = particle size in interval i (Eqs. 42 and 43), m
D_L = diffusivity, $m^2 \cdot s^{-1}$
f = fraction of fines removal stream fed to the dissolver, dimensionless
f_a = fraction of filter area available for washing and deliquoring, dimensionless
f_i = number fraction of particles in size interval i (Eqs. 42 and 43), dimensionless
F_S = mass flow rate of solids in dryer, $kg \cdot s^{-1}$
g = gravity constant, 9.81 $m \cdot s^{-2}$; order of growth rate with respect to supersaturation, dimensionless
G = growth rate, $m \cdot s^{-1}$
G_{ic} = critical growth rate for impurity inclusion, $m \cdot s^{-1}$
H = Heaviside function
j = order of nucleation rate constant with respect to magma density, dimensionless
k = permeability, m^2
k_a = surface-area shape factor, dimensionless
k_b = constant in nucleation kinetics equation, $no \cdot (kg\ solvent)^{-1} \cdot s^{-1} \cdot (kg \cdot kg\ solvent^{-1})^{-b}$
k_c = constant cooling rate, $°C \cdot s^{-1}$
k_d = constant MSA addition rate, $kg \cdot s^{-1}$
k_e = constant evaporation rate, $kg\ solvent \cdot s^{-1}$
k_g = constant in growth kinetics equation, $m \cdot s^{-1} \cdot (kg \cdot kg\ solvent^{-1})^{-g}$
k_{im} = constant in impurity inclusion equation, $kg \cdot kg^{-1} \cdot s^n \cdot m^{-(m+n)}$
k_L = constant in size-dependent growth rate equation, m^{-1}
k_r = reaction constant, $s^{-1} \cdot (kg \cdot kg\ solvent^{-1})^{1-n}$
k_v = volume shape factor, dimensionless
l = order of growth rate with respect to size, dimensionless
L = crystal size, m
L_c = largest size to be recycled back to the crystallizer from the product classifier, m
L_f = largest size to be removed by the fines removal stream, m
L_s = size of seed particles, m

L_0 = size of nuclei, m
m = order of particle size in impurity inclusion equation, dimensionless
m_A = amount of mass separating agent, kg
m_L = amount of solvent, kg
m_s = mass of seed crystals, kg
mC_p = heat capacity, $J \cdot K^{-1}$
M_i = ith moment of distribution, m^i
M_T = magma density, $kg \cdot m^{-3}$
n = order of growth rate in impurity inclusion equation, dimensionless; population density, $no \cdot m^{-4}$
N = impeller speed, rpm
N_{Ca} = capillary number, dimensionless
N_D = dispersion number, dimensionless
N_{Nu} = nucleation number, dimensionless
N_{Gr} = growth number, dimensionless
N_W = wash ratio, dimensionless
p = power of concentration in reaction kinetics, dimensionless
Δp = vacuum level or pressure difference, $N \cdot m^{-2}$
Q_f = crystallizer feed volumetric flow rate, $m^3 \cdot s^{-1}$
Q_p = crystallizer product volumetric flow rate, $m^3 \cdot s^{-1}$
Q_o = volumetric flow rate of the fines removal stream, $m^3 \cdot s^{-1}$
Q_u = volumetric flow rate of the feed to the particle classifier, $m^3 \cdot s^{-1}$
q_f = filtrate volumetric flow rate, $m^3 \cdot s^{-1}$
r_0, r_1 = filter cake radius in centrifugal filter (Figure 2b), m
r_d = drying rate at constant rate period, $kg \cdot m^{-2} \cdot s^{-1}$
R = ratio of removal rates of particles of size less than L_f to those greater than L_f
R_m = filter medium resistance, m^{-1}
S = saturation, dimensionless
S_R = reduced saturation, dimensionless
S_∞ = irreducible saturation, dimensionless
t = time, s
t_a = time available (for washing and deliquoring), s
t_d = time required for deliquoring, s
t_{dry} = time required for drying, s
t_f = time required for filtration, s
t_w = time required for washing, s
T = solution temperature, °C
T_m = heat-transfer medium temperature, °C
U = heat-transfer coefficient, $J \cdot m^{-2} \cdot s^{-1} \cdot K^{-1}$
V = crystallizer volume, m^3
V_f = volume of filtrate, m^3
W_S = mass of solids in dryer, kg
x = order of cooling (Eq. 44), dimensionless
X = moisture content, kg liquid·(kg solid)$^{-1}$
y = fraction of solute remaining in filter cake after washing, dimensionless
Z = ratio of withdrawal rates of particles of size greater than L_c to those less than L_c

Greek letters

δ = cake thickness, m
ϵ = porosity, dimensionless; specific power input, W·(kg solution)$^{-1}$
μ = viscosity, $kg \cdot m^{-1} \cdot s^{-1}$
ρ = density, $kg \cdot m^{-3}$
σ = surface tension, $N \cdot m^{-1}$
λ = parameter (defined in Eq. 30), dimensionless
ψ = angle of submergence, rad
ω = angular velocity, $rad \cdot s^{-1}$

Subscripts

c = critical
f = final
i = index
L = liquid
S = solid
0 = initial

Literature Cited

Abegg, C. F., J. D. Stevens, and M. A. Larson, "Crystal Size Distributions in Continuous Crystallizers When Growth Rate is Size Dependent," *AIChE J.*, **14**, 118 (1968).

Bamforth, A. W., *Industrial Crystallization*, Leonard Hill, London (1965).

Bermingham, S. K., A. M. Neumann, H. J. M. Kramer, P. J. T. Verheijen, G. M. van Rosmalen, and J. Grievink, "A Design Procedure and Predictive Models for Solution Crystallisation Processes," *AIChE Symp. Ser. No. 323*, **96**, 250 (2000).

Berry, D. A., and K. M. Ng, "Separation of Quaternary Conjugate Salt Systems by Fractional Crystallization," *AIChE J.*, **42**, 2162 (1996).

Berry, D. A., and K. M. Ng, "Synthesis of Reactive Crystallization Processes," *AIChE J.*, **43**, 1737 (1997).

Berry, D. A., S. R. Dye, and K. M. Ng, "Synthesis of Drowning-Out Crystallization-Based Separations," *AIChE J.*, **43**, 91 (1997).

Bohlin, M., and Å. C. Rasmuson, "Application of Controlled Cooling and Seeding in Batch Crystallization," *Can. J. Chem. Eng.*, **70**, 120 (1992).

Botsaris, G. D., E. A. Mason, and R. C. Reid, "Incorporation of Ionic Impurities in Crystals Growing from Solution. The Case of Lead Ions in Potassium Chloride Crystals," *AIChE J.*, **13**, 764 (1967).

Brooks, R., A. T. Horton, and J. L. Torgesen, "Occlusion of Mother Liquor in Solution-Grown Crystals," *J. Cryst. Growth*, **2**, 279 (1968).

Bruton, J. A., R. C. Prim, and W. P. Slichter, "The Distributions of Solute in Crystals Grown from the Melt," *J. Chem. Phys.*, **21**, 1987 (1953).

Chang, W.-C., PhD Diss., Univ. of Massachusetts, Amherst (1998).

Chang, W.-C., and K. M. Ng, "Synthesis of the Processing System Around a Crystallizer," *AIChE J.*, **44**, 2240 (1998).

Chianese, A., S. Di Cave, and B. Mazzarotta, "Investigation on Some Operating Factors Influencing Batch Cooling Crystallization," *Industrial Crystallization 84*, S. J. Jančić and E. J. de Jong, eds., Elsevier, Amsterdam (1984).

Chung, S. H., D. L. Ma, and R. D. Braatz, "Optimal Seeding in Batch Crystallization," *Can. J. Chem. Eng.*, **77**, 590 (1999).

Cisternas, L. A., and D. F. Rudd, "Process Designs for Fractional Crystallization from Solution," *Ind. Eng. Chem. Res.*, **32**, 1993 (1993).

Denbigh, K. T., and E. T. White, "Studies on Liquid Inclusions in Crystals," *Chem. Eng. Sci.*, **21**, 739 (1966).

Dye, S. R., and K. M. Ng, "Bypassing Eutectics with Extractive Crystallization: Design Alternatives and Tradeoffs," *AIChE J.*, **41**, 1456 (1995a).

Dye, S. R., and K. M. Ng, "Fractional Crystallization: Design Alternatives and Tradeoffs," *AIChE J.*, **41**, 2427 (1995b).

Garside, J., and M. B. Shah, "Crystallization Kinetics from MSMPR Crystallizers," *Ind. Eng. Chem. Process Des. Dev.*, **19**, 509 (1980).

Garside, J., "Industrial Crystallization from Solution," *Chem. Eng. Sci.*, **40**, 3 (1985).

Genck, W. J., "Crystallization from Solutions," *Handbook of Separation Techniques for Chemical Engineers*, 3rd ed., P. A. Schweitzer, ed., McGraw-Hill, New York (1997).

Genck, W. J., "Better Growth in Batch Crystallizers," *Chem. Eng.*, **107**(8), 90 (2000).

Grootscholten, P. A. M., C. J. Asselbergs, and E. J. De Jong, "Secondary Nucleation," *Industrial Crystallization 81*, S. J. Jančić and E. J. de Jong, eds., North-Holland, Amsterdam (1982).

Green, D. A., Personal Communication (2000).

Hall, R. N., "Segregation of Impurities During the Growth of Germanium and Silicon Crystals," *J. Phys. Chem.*, **57**, 836 (1953).

Heffels, S. K., E. J. de Jong, and M. Nienoord, "Improved Operation and Control of Batch Crystallizers," *AIChE Symp. Ser. No. 284*, **87**, 170 (1991).

Hill, P. J., and K. M. Ng, "Simulation of Solids Processes Accounting for Particle-Size Distribution," *AIChE J.*, **43**, 715 (1997).

Jagadesh, D., N. Kubota, M. Yokota, A. Sato, and N. S. Tavare, "Large and Mono-Sized Product Crystals from Natural Cooling Mode Batch Crystallizer," *J. Chem. Eng. Jpn.*, **29**, 865 (1996).

Jagadesh, D., N. Kubota, M. Yokota, N. Doki, and A. Sato, "Seeding Effect on Batch Crystallization of Potassium Sulfate under Natural

Cooling Mode and a Simple Design Method of Crystallizer," *J. Chem. Eng. Jpn.*, **32**, 514 (1999).
Jančić, S. J., and P. A. M. Grootscholten, *Industrial Crystallization*, Delft Univ. Press, Reidel, Dordrecht (1984).
Jones, A. G., and J. W. Mullin, "Programmed Cooling Crystallization of Potassium Sulphate Solutions," *Chem. Eng. Sci.*, **29**, 105 (1974).
Jones, A. G., "Crystallization and Downstream Processing Interactions," *Powtech '85, Particle Technology*, Institution of Chemical Engineers, Birmingham, p. 1 (1985).
Jones, A. G., A. Chianese, and J. W. Mullin, "Effect of Fines Destruction on the Batch Cooling Crystallization of Potassium Sulphate," *Industrial Crystallization 84*, S. J. Jančić and E. J. de Jong, eds., Elsevier, Amsterdam (1984).
Jones, A. G., J. Budz, and J. W. Mullin, "Batch Crystallization and Solid-Liquid Separation of Potassium Sulphate," *Chem. Eng. Sci.*, **42**, 619 (1987).
Kelkar, V. V., and K. M. Ng, "Design of Reactive Crystallization Systems Incorporating Kinetics and Mass-Transfer Effects," *AIChE J.*, **45**, 69 (1999).
Koros, W. J., D. A. Dalrymple, R. P. Kuhlman, and N. F. Brockmeir, "Crystallization of Sodium Chloride in a Continuous Mixed Suspension Crystallizer," *AIChE Symp. Ser. No. 121*, **68**, 67 (1972).
Kroschwitz, J. I., and M. Howe-Grant, eds., *Kirk-Othmer Encyclopedia of Chemical Technology*, Vol. 1, 4th ed., Wiley, New York, p. 466 (1991).
Kurihara, K., S. Miyashita, G. Sazaki, T. Nakada, S. D. Durbin, H. Komatsu, T. Ohba, and K. Ohki, "Incorporation of Impurity to a Tetragonal Lysozyme Crystal," *J. Crystal Growth*, **196**, 285 (1999).
Lang, Y., A. M. Cervantes, and L. T. Biegler, "Dynamic Optimization of a Batch Cooling Crystallization Process," *Ind. Eng. Chem. Res.*, **38**, 1469 (1999).
Larson, M. A., and A. D. Randolph, "Size Distribution Analysis in Continuous Crystallization," *Chem. Eng. Prog. Symp. Ser. No. 95*, **65**, 1 (1969).
Larson, M. A., and J. Garside, "Crystallizer Design Techniques Using the Population Balance," *Chem. Eng. (London)*, **274**, 318 (1973).
Liu, C. H., D. H. Zhang, C. G. Sun, and Z. Q. Shen, "The Modelling and Simulation of a Multistage Crystallizer," *Chem. Eng. J.*, **46**, 9 (1991).
MacDonald, M. J., C. F. Chu, P. P. Guilloit, and K. M. Ng, "A Generalized Blake-Kozeny Equation for Multisized Spherical Particles," *AIChE J.*, **37**, 1583 (1991).
Mackintosh, D. L., and E. T. White, "The Formation of Inclusions in Sugar Crystals," *AIChE Symp. Ser. No. 153*, **72**, 11 (1976).
Mahajan, A. J., C. J. Orella, and D. J. Kirwan, "Analysis of Size Distribution and Growth Kinetics during the Batch Crystallization of L-Asparagine," *AIChE Symp. Ser. No. 284*, **87**, 143 (1991).
Marshall, W. R., Jr., "Atomization and Spray Drying," *Chem. Eng. Prog. Monog. Ser.*, **50**, 1 (1954).
McCabe, W. L., J. C. Smith, and P. Harriott, *Unit Operations of Chemical Engineering*, 5th ed., McGraw-Hill, New York (1993).
McCrone, W. C., "Polymorphism," *Physics and Chemistry of the Organic Solid State*, D. Fox, M. M. Labes, and A. Weissberger, eds., Wiley-Interscience, New York (1965).
Mersmann, A., and M. Kind, "Chemical Engineering Aspects of Precipitation from Solution," *Chem. Eng. Technol.*, **11**, 264 (1988).
Moore, W. P., "Optimize Batch Crystallization," *Chem. Eng. Prog.*, **90**(9), 73 (1994).
Mullin, J. W., *Crystallization*, 3rd ed., Butterworth-Heinemann, Oxford (1993).
Mullin, J. W., and J. Nývlt, "Programmed Cooling of Batch Crystallizers," *Chem. Eng. Sci.*, **26**, 369 (1971).
Myerson, A. S., ed., *Handbook of Industrial Crystallization*, Butterworth-Heinemann, Boston (1993).
Myerson, A. S., S. E. Decker, and W. Fan, "Solvent Selection and Batch Crystallization," *Ind. Eng. Chem. Process Des. Dev.*, **25**, 925 (1986).
Nonhebel, G., and A. A. H. Moss, *Drying of Solids in the Chemical Industry*, Butterworths, London (1971).
Nývlt, J., O. Söhnel, M. Matuchová, and M. Broul, *The Kinetics of Industrial Crystallization*, Elsevier, Amsterdam (1985).
Nývlt, J., *Design of Crystallizers*, CRC Press, Boca Raton, FL (1992).
Oldshue, J. Y., "Agitation and Mixing," *Handbook of Industrial Crystallization*, A. S. Myerson, ed., Butterworth-Heinemann, Newton, MA, p. 165 (1993).
Ouchiyama, N., and T. Tanaka, "Porosity Estimation for Random Packings of Spherical Particles," *Ind. Eng. Chem. Fundam.*, **23**, 490 (1984).
Pietsch, W., *Size Enlargement by Agglomeration*, John Wiley, Chichester (1991).
Rajagopal, S., K. M. Ng, and J. M. Douglas, "Design of Solids Processes: Production of Potash," *Ind. Eng. Chem. Res.*, **27**, 2071 (1988).
Randolph, D. A., G. L. Beer, and J. P. Keener, "Stability of the Class II Classified Product Crystallizer with Fines Removal," *AIChE J.*, **19**, 1140 (1973).
Randolph, D. A., and M. A. Larson, *Theory of Particulate Process*, 2nd ed., Academic Press, San Diego (1988).
Rossiter, A. P., and J. M. Douglas, "Design and Optimisation of Solids Processes: 2. Optimisation of Crystalliser, Centrifuge, and Drying Systems," *Chem. Eng. Res. Dev.*, **64**, 184 (1986).
Rouault, Y., and S. Assouline, "A Probabilistic Approach Towards Modeling the Relationships Between Particle and Pore Size Distributions: The Multicomponent Packed Sphere Case," *Powder Technol.*, **96**, 33 (1998).
Rousseau, R. W., ed., *Handbook of Separation Process Technology*, Wiley, New York (1987).
Schroer, J. W., C. Wibowo, and K. M. Ng, "Synthesis of Chiral Crystallization Processes," *AIChE J.*, **47**, 369 (2001).
Sherwin, M. B., R. Shinnar, and S. Katz, "Dynamic Behavior of the Well-Mixed Isothermal Crystallizer," *AIChE J.*, **13**, 1141 (1967).
Slaminko, P., and A. S. Myerson, "The Effect of Crystal Size on Occlusion Formation During Crystallization from Solution," *AIChE J.*, **27**, 1029 (1981).
Sohnel, O., and J. Garside, *Precipitation Basic Principles and Industrial Applications*, Butterworth-Heinemann, Oxford (1992).
Takano, K., R. Gani, T. Ishikawa, and P. Kolar, "Integrated System for Design and Analysis of Industrial Processes with Electrolyte System," Paper presented in Escape '99, Budapest, Hungary (1999).
Tavare, S. N., "Batch Crystallizers," *Rev. Chem. Eng.*, **7**, 211 (1991).
Tavare, S. N., *Industrial Crystallization: Process Simulation Analysis and Design*, Plenum Press, New York (1995).
Wakeman, R. J., "The Performance of Filtration Post-Treatment Processes: 1. The Prediction and Calculation of Cake Dewatering Characteristics," *Filtr. Sep.*, **16**, 655 (1979).
Wakeman, R. J., "The Performance of Filtration Post-Treatment Processes: 2. The Estimation of Cake Washing Characteristics," *Filtr. Sep.*, **17**, 67 (1980).
Wakeman, R. J., and E. S. Tarleton, *Filtration: Equipment Selection, Modeling and Process Simulation*, Elsevier, Oxford (1999).
White, E. T., L. L. Bendig, and M. A. Larson, "The Effect of Size on the Growth Rate of Potassium Sulfate Crystals," *AIChE Symp. Ser. No. 153*, **72**, 41 (1976).
Wibowo, C., and K. M. Ng, "Synthesis of Bulk Solids Processing Systems," *AIChE J.*, **45**, 1629 (1999).
Wibowo, C., and K. M. Ng, "Unified Approach for Synthesizing Crystallization-Based Separation Processes," *AIChE J.*, **46**, 1400 (2000).
Wibowo, C., and K. M. Ng, "Operational Problems in Solids Processing Plants: a Systems View," *AIChE J.*, **47**, 107 (2001).
Yu, K. M., and J. M. Douglas, "Self-Generated Oscillations in Continuous Crystallizers: Part I. Analytical Prediction of the Oscillating Output," *AIChE J.*, **21**, 917 (1975).
Zeitsch, K., "Centrifugal Filtration," *Solid-Liquid Separation*, 2nd ed., L. Svarovsky, ed., Butterworths, London, p. 368 (1981).

Manuscript received Oct. 17, 2000, and revision received May 7, 2001.